

<sup>1</sup> The human visual system preserves the hierarchy  
<sup>2</sup> of 2-dimensional pattern regularity

<sup>3</sup> Peter J. Kohler<sup>1,2,3</sup> and Alasdair D. F. Clarke<sup>4</sup>

<sup>4</sup> *<sup>1</sup> York University, Department of Psychology, Toronto, ON M3J 1P3, Canada*

<sup>5</sup> *<sup>2</sup> Centre for Vision Research, York University, Toronto, ON, M3J 1P3, Canada*

<sup>6</sup> *<sup>3</sup>Stanford University, Department of Psychology, Stanford, CA 94305, United States*

<sup>7</sup> *<sup>4</sup>University of Essex, Department of Psychology, Colchester, UK, CO4 3SQ*

<sup>8</sup> **Abstract**

Symmetries are present at many scales in images of natural scenes. Humans and other animals are highly sensitive to visual symmetry, and a large literature has demonstrated contributions of symmetry to numerous domains of visual perception. The four fundamental symmetries, reflection, rotation, translation and glide reflection, can be combined in exactly 17 distinct ways. These *wallpaper groups* represent the complete set of symmetries in 2D images and have recently found use in the vision science community as an ideal stimulus set for studying the perception of symmetries in textures. The goal of the current study is to provide a more comprehensive description of responses to symmetry in the human visual system, by collecting both brain imaging (Steady-State Visual Evoked Potentials measured using high-density EEG) and behavioral (symmetry detection thresholds) data using the entire set of wallpaper groups. This allows us to probe the hierarchy of complexity among wallpaper groups, in which simpler groups are subgroups of more complex ones. We find that this hierarchy is preserved almost perfectly in both behavior and brain activity: A multi-level Bayesian GLM indicates that for most of the 63 subgroup relationships, subgroups produce lower amplitude responses in visual cortex (posterior probability: > 0.95 for 56 of 63) and require longer presentation durations to be reliably detected (posterior probability: > 0.95 for 48 of 63). This systematic pattern is seen only in visual cortex and only in components of the brain response known to be symmetric-specific. Our results show that representations of symmetries in the human brain are precise and rich in detail, and that this precision is reflected in behavior. These findings expand our understanding of symmetry perception, and open up new avenues for research on how fine-grained representations of regular textures contribute to natural vision.

Symmetries are abundant in natural and man-made environments, due to a complex interplay of physical forces that govern pattern formation in nature. Sensitivity to symmetry has been demonstrated in a number of species, includes bees (Giurfa et al., 1996), fish (Morris and Casey, 1998; Schlüter et al., 1998), birds (Møller, 1992; Swaddle and Cuthill, 1994) and dolphins (von Fersen et al., 1992), and may be used as a cue for mate selection in many species (Swaddle, 1999) including humans (Rhodes et al., 1998). Humans cultures have created and appreciated symmetrical patterns throughout history, and since the gestalt movement of the early 20th century, symmetry has been recognized as important for visual perception. Symmetry contributes

38 to the perception of shapes (Palmer, 1985; Li et al., 2013), scenes (Apthorp and Bell, 2015) and  
39 surface properties (Cohen and Zaidi, 2013). This literature is almost exclusively based on stimuli  
40 in which one or more symmetry axes are placed at a single point in the image. Focus has been  
41 on mirror symmetry or reflection, with relatively few studies including the other fundamental  
42 symmetries: rotation, translation and glide reflection (Wagemans, 1998) - perhaps because reflection  
43 has been found to be more perceptually salient (Mach, 1959; Royer, 1981; Palmer, 1991; Ogden  
44 et al., 2016; Hamada and Ishihara, 1988) and produce more brain activity (Makin et al., 2013, 2014,  
45 2012; Wright et al., 2015). In the current study, we take a different approach by investigating  
46 visual processing of regular textures in which combinations of the four fundamental symmetries  
47 tile the 2D plane.

48 In the two spatial dimensions relevant for images, symmetries can be combined in 17 distinct  
49 ways, the *wallpaper groups* (Fedorov, 1891; Polya, 1924; Liu et al., 2010). Previous work on a subset  
50 of four of the wallpaper groups used functional MRI to demonstrate that rotation symmetries  
51 in wallpapers elicit parametric responses in several areas in occipital cortex, beginning with  
52 visual area V3 (Kohler et al., 2016). This effect was also robust when symmetry responses were  
53 measured with electroencephalography (EEG) using both Steady-State Visual Evoked Potentials  
54 (SSVEPs)(Kohler et al., 2016) and Event-Related Potentials (Kohler et al., 2018). The SSVEP  
55 technique uses periodic visual stimulation to produce a periodic brain response that is confined to  
56 integer multiples of the stimulation frequency known as harmonics. SSVEP response harmonics  
57 can be isolated in the frequency domain and depending on the specific design, different harmonics  
58 will express different aspects of the brain response. (Norcia et al., 2015). Here we extend on the  
59 previous work by collecting SSVEPs and psychophysical data from human participants viewing  
60 the full set of wallpaper groups. We measure responses in visual cortex to 16 out of the 17  
61 wallpaper groups, with the 17th serving as a control stimulus. Our goal is to provide a more  
62 complete picture of how wallpaper groups are represented in the human visual system.

63 A wallpaper group is a topologically discrete group of isometries of the Euclidean plane, i.e.  
64 transformations that preserve distance (Liu et al., 2010). The wallpaper groups differ in the  
65 number and kind of these transformations and we can uniquely refer to different groups using  
66 crystallographic notation. In brief, most groups are notated by  $PXZ$ , where  $X \in \{1, 2, 3, 4, 6\}$   
67 indicates the highest order of rotation symmetry and  $Z \in \{m, g\}$  indicates whether the pattern  
68 contains reflection (m) or glide reflection (g). For example,  $P4$  contains 4 fold rotation, while  
69  $P4MM$  contains 4 fold rotation and two mirror reflections. By convention, many of the groups  
70 are given shortened names: for example,  $P4MM$  is usually referred to as  $P4M$ , as the second  
71 reflection can be deduced from the presence of a 4 fold rotation alongside a reflection. (see  
72 Figures 1 and 2 for examples). Two of the groups start with a  $C$  rather than a  $P$ , ( $CM$  and  $CMM$ )  
73 which indicates that the symmetries are specified relative to a cell that itself contains repetition.  
74 Full details of the naming convention and examples of the wallpaper groups can be found on  
75 wikipedia.

76 In mathematical group theory, when the elements of one group is completely contained in  
77 another, the inner group is called a subgroup of the outer group (Liu et al., 2010). The full list  
78 of subgroup relationships is listed in Section 1.4.2 of the Supplementary Material. Subgroup

79 relationships between wallpaper groups can be distinguished by their indices. The index of a  
 80 subgroup relationship is the number of cosets, i.e. the number of times the subgroup is found  
 81 in the supergroup (Liu et al., 2010). As an example, let us consider groups  $P_2$  and  $P_6$  (see Figure  
 82 1C). If we ignore the translations in two directions that both groups share, group  $P_6$  consists of  
 83 the set of rotations  $\{0^\circ, 60^\circ, 120^\circ, 180^\circ, 240^\circ, 300^\circ\}$ , in which  $P_2 \{0^\circ, 180^\circ\}$  is contained.  
 84  $P_2$  is thus a subgroup of  $P_6$ , and  $P_6$  can be generated by combining  $P_2$  with rotations  $\{0^\circ, 120^\circ, 240^\circ\}$ .  
 85 Because  $P_2$  is repeated three times in  $P_6$ ,  $P_2$  is a subgroup of  $P_6$  with index 3 (Liu et al., 2010).  
 86 A more complex example are the subgroups of  $PMM$ , which is made up of two reflections, and  
 87 a rotation of  $180^\circ$ . As such,  $P_2$  and  $PM$  are both subgroups of  $PMM$ . (Illustrative examples are  
 88 given in Figure 1) The 17 wallpaper groups thus obey a hierarchy of complexity where simpler  
 89 groups are subgroups of more complex ones (Coxeter and Moser, 1972).

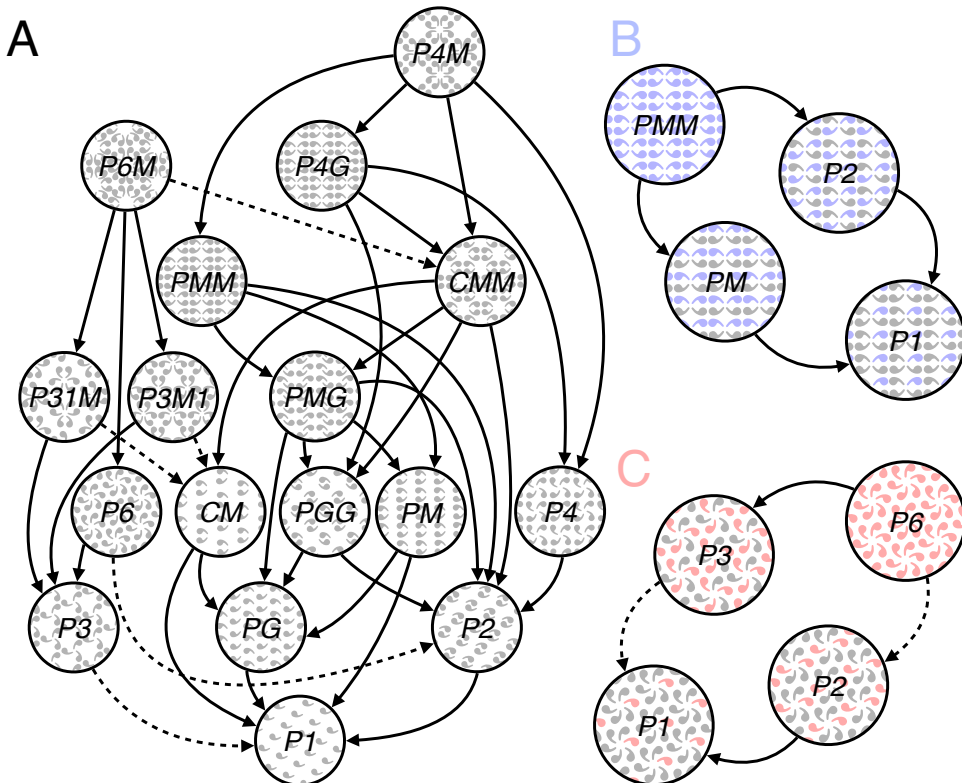


Figure 1: Subgroup relationships with indices 2 (solid lines) and 3 (dashed line) are shown in (A). All other relationships can be inferred by identifying the shortest path through the hierarchy, and multiplying the subgroup indices. For example,  $P_1$  is related to  $P_6$  through  $P_6 \rightarrow P_3$  (index 2) and  $P_3 \rightarrow P_1$  (index 3) so  $P_1$  is also a subgroup of  $P_6$  with index  $3 \times 2 = 6$ . We also show enlarged versions of some of the subgroup relationships involving  $PMM$  (B, shown in blue) and  $P_6$  (C, shown in red) and highlight the symmetries within the subgroups to emphasize how the supergroup can be generated by adding additional transformations to the subgroup.

90 The two datasets we present here make it possible to assess the extent to which both behavior  
 91 and brain responses follow the hierarchy of complexity expressed by the subgroup relationships.  
 92 Based on previous brain imaging work showing that patterns with more axes of symmetry pro-  
 93 duce greater activity in visual cortex (Sasaki et al., 2005; Tyler et al., 2005; Kohler et al., 2018,  
 94 2016; Keefe et al., 2018), we hypothesized that more complex groups would produce larger SSVEPs.

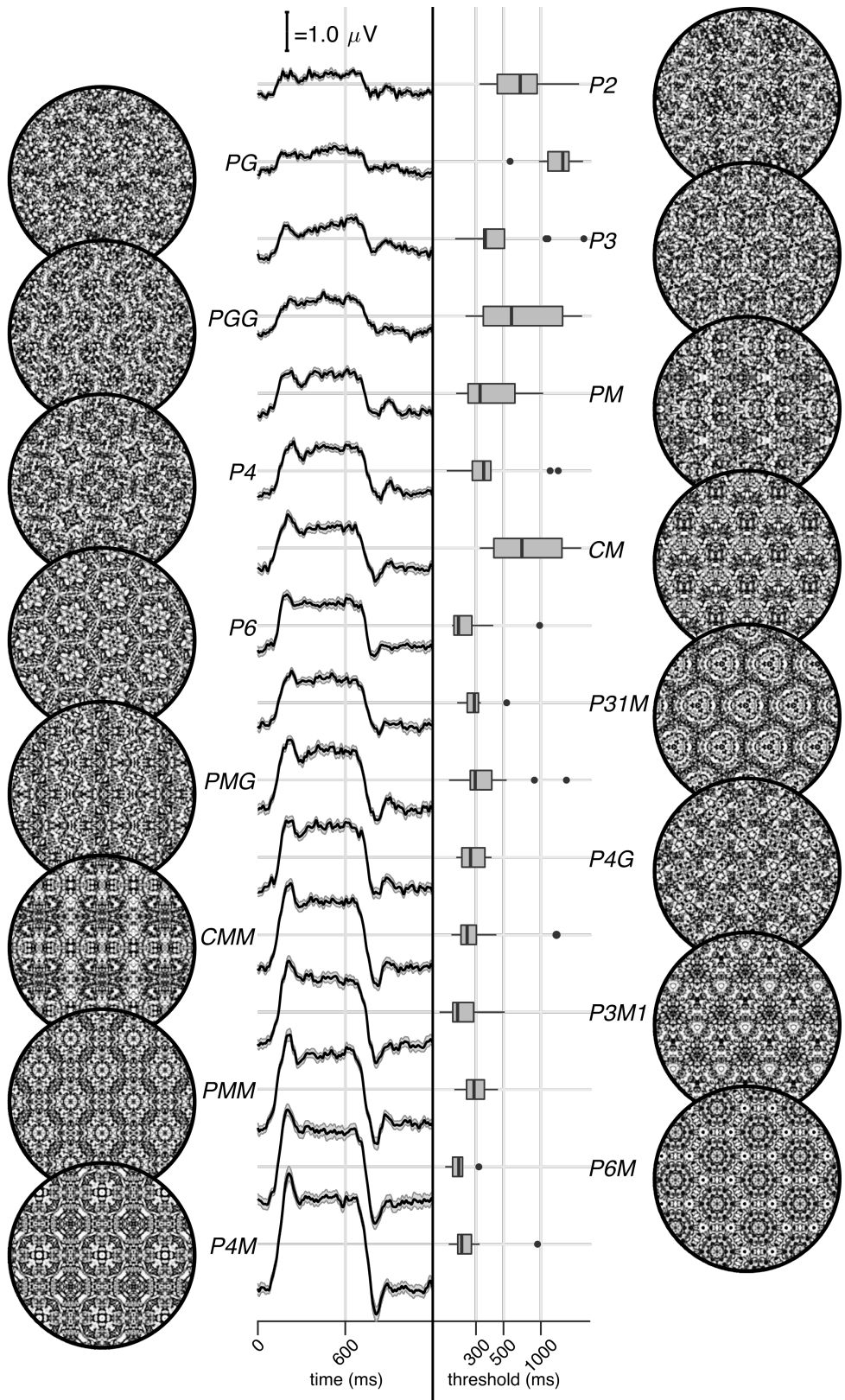


Figure 2: Examples of each of the 16 wallpaper groups are shown in the left- and right-most column of the figures, next to the corresponding SSVEP (center-left) and psychological (center-right) data from each group. The SSVEP data are odd-harmonic-filtered cycle-average waveforms. In each cycle, a  $P_1$  exemplar was shown for the first 600 ms, followed by the original exemplar for the last 600 ms. Errorbars are standard error of the mean. Psychophysical data are presented as boxplots reflecting the distribution of display duration thresholds. The 16 groups are ordered by the strength of the SSVEP response, to highlight the range of response amplitudes.

95 For the psychophysical data, we hypothesized that more complex groups would lead to shorter  
96 symmetry detection thresholds, based on previous data showing that under a fixed presentation  
97 time, discriminability increases with the number of symmetry axes in the pattern (Wagemans  
98 et al., 1991). Our results confirm both hypotheses, and show that activity in human visual cortex  
99 is remarkably consistent with the hierarchical relationships between the wallpaper groups, with  
100 SSVEP amplitudes and psychophysical thresholds following these relationships at a level that is  
101 far beyond chance. The human visual system thus appears to encode all of the fundamental sym-  
102 metries using a representational structure that closely approximates the subgroup relationships  
103 from group theory.

## 104 Results

105 The stimuli used in our two experiments were generated from random-noise textures, which  
106 made it possible to generate multiple exemplars from each of the wallpaper groups, as described  
107 in detail elsewhere (Kohler et al., 2016). We generated control stimuli matched to each exemplar  
108 in the main stimulus set, by scrambling the phase but maintaining the power spectrum. All  
109 wallpaper groups are inherently periodic because of their repeating lattice structure. Phase  
110 scrambling maintains this periodicity, so the phase-scrambled control images all belong to group  
111  $P_1$  regardless of group membership of the original exemplar.  $P_1$  contains no symmetries other  
112 than translation, while all other groups contain translation in combination with one or more of the  
113 other three fundamental symmetries (reflection, rotation, glide reflection) (Liu et al., 2010). In our  
114 SSVEP experiment, this stimulus set allowed us to isolate brain activity specific to the symmetry  
115 structure in the exemplar images from activity associated with modulation of low-level features,  
116 by alternating exemplar images and control exemplars. In this design, responses to structural  
117 features beyond the shared power spectrum, including any symmetries other than translation,  
118 are isolated in the odd harmonics of the image update frequency (Kohler et al., 2016; Norcia et al.,  
119 2015, 2002). Thus, the combined magnitude of the odd harmonic response components can be  
120 used as a measure of the overall strength of the visual cortex response.

121 The psychophysical experiment took a distinct but related approach. In each trial an exemplar  
122 image was shown with its matched control, one image after the other, and the order varied pseudo-  
123 randomly such that in half the trials the original exemplar was shown first, and in the other half  
124 the control image was shown first. After each trial, participants were instructed to indicate  
125 whether the first or second image contained more structure. The duration of both images was  
126 controlled by a staircase procedure so that a threshold duration for symmetry detection could be  
127 computed for each wallpaper group.

128 Examples of the wallpaper groups and a summary of our brain imaging and psychophysical  
129 measurements are shown in Figure 2. For our primary SSVEP analysis, we only considered EEG  
130 data from a pre-determined region-of-interest (ROI) consisting of six electrodes over occipital cor-  
131 tex (see Supplementary Figure 1.1). SSVEP data from this ROI was filtered so that only the odd  
132 harmonics that capture the symmetry response contribute to the waveforms. While waveform am-  
133 plitude is quite variable among the 16 groups, all groups have a sustained negative-going response

134 that begins at about the same time for all groups, 180 ms after the transition from the  $P_1$  control  
135 exemplar to the original exemplar. To reduce the amplitude of the symmetry-specific response to  
136 a single number that could be used in further analyses and compared to the psychophysical data,  
137 we computed the root-mean-square (RMS) over the odd-harmonic-filtered waveforms. The data  
138 in Figure 2 are shown in descending order according to RMS. The psychophysical results, shown  
139 in box plots in Figure 2, were also quite variable between groups, and there seems to be a general  
140 pattern where wallpaper groups near the top of the figure, that have lower SSVEP amplitudes,  
141 also have longer psychophysical threshold durations.

142 We now wanted to test our two hypotheses about how SSVEP amplitudes and threshold du-  
143 rations would follow subgroup relationships, and thereby quantify the degree to which our two  
144 measurements were consistent with the group theoretical hierarchy of complexity. We tested  
145 each hypothesis using the same approach. We first fitted a Bayesian model with wallpaper group  
146 as a factor and participant as a random effect. We fit the model separately for SSVEP RMS and  
147 psychophysical data and then computed posterior distributions for the difference between su-  
148 pergroup and subgroup. These difference distributions allowed us to compute the conditional  
149 probability that the supergroup would produce (a) larger RMS and (b) a shorter threshold du-  
150 rations, when compared to the subgroup. The posterior distributions are shown in Figure 3 for  
151 the SSVEP data, and in Figure 4 for the psychophysical data, which distributions color-coded  
152 according to conditional probability. For both data sets our hypothesis is confirmed: For the  
153 overwhelming majority of the 63 subgroup relationships, supergroups are more likely to produce  
154 larger symmetry-specific SSVEPs and shorter symmetry detection threshold durations, and in  
155 most cases the conditional probability of this happening is extremely high.

156 We also ran a control analysis using (1) odd-harmonic SSVEP data from a six-electrode ROI  
157 over parietal cortex (see Supplementary Figure 1.1) and (2) even-harmonic SSVEP data from the  
158 same occipital ROI that was used in our primary analysis. By comparing these two control  
159 analysis to our primary SSVEP analysis, we can address the specify of our effects in terms of  
160 location (occipital cortex vs parietal cortex) and harmonic (odd vs even). For both control analyses  
161 (plotted in Supplementary Figures 3.3 and 3.4), the correspondence between data and subgroup  
162 relationships was substantially weaker than in the primary analysis. We can quantify the strength  
163 of the association between the data and the subgroup relationships, by asking what proportion of  
164 subgroup relationships that reach or exceed a range of probability thresholds. This is plotted in  
165 Figure 5, for our psychophysical data, our primary SSVEP analysis and our two control SSVEP  
166 analyses. It shows that odd-harmonic SSVEP data from the occipital ROI and symmetry detection  
167 threshold durations both have a strong association with the subgroup relationships such that a  
168 clear majority of the subgroups survive even at the highest threshold we consider ( $p(\Delta > 0 | data) >$   
169 0.99). The association is far weaker for the two control analyses.

170 SSVEP data from four of the wallpaper groups ( $P_2$ ,  $P_3$ ,  $P_4$  and  $P_6$ ) was previously published  
171 as part of our earlier demonstration of parametric responses to rotation symmetry in wallpaper  
172 groups(Kohler et al., 2016). We replicate that result using our Bayesian approach, and find an  
173 analogous parametric effect in the psychophysical data (see Supplementary Figure 4.1). We also  
174 conducted an analysis testing for an effect of index in our two datasets and found that subgroup

relationships with higher indices tended to produce greater pairwise differences between the subgroup and supergroup, for both SSVEP RMS and symmetry detection thresholds (see Supplementary Figure 4.2). The effect of index is relatively weak, but the fact that there is a measurable index effect can nonetheless be taken as preliminary evidence that representations of symmetries in wallpaper groups may be compositional.

Finally, we conducted a correlation analysis comparing SSVEP and psychophysical data and found a reliable correlation ( $R^2 = 0.44$ , Bayesian confidence interval [0.28, 0.55]). The correlation reflects an inverse relationship: For subgroup relationships where the supergroup produces a much *larger* SSVEP amplitude than the subgroup, the supergroup also tends to produce a much *smaller* symmetry detection threshold. This is consistent with our hypotheses about how the two measurements relate to symmetry representations in the brain, and suggests that our brain imaging and psychophysical measurements are at least to some extent tapping into the same underlying mechanisms.

## Discussion

Here we show that beyond merely responding to the elementary symmetry operations of reflection (Sasaki et al., 2005; Tyler et al., 2005) and rotation (Kohler et al., 2016), the visual system represents the hierarchical structure of the 17 wallpaper groups, and thus every combination of the four fundamental symmetries (rotation, reflection, translation, glide reflection) which comprise the set of regular textures. Both SSVEP amplitudes and symmetry detection thresholds preserve the hierarchy of complexity among the wallpaper groups that is captured by the subgroup relationships (Coxeter and Moser, 1972). For the SSVEP, this remarkable consistency was specific to the odd harmonics of the stimulus frequency that are known to capture the symmetry-specific response (Kohler et al., 2016) and to electrodes in a region-of-interest (ROI) over occipital cortex. When the same analysis was done using the odd harmonics from electrodes over parietal cortex (Supplementary Figure 3.3) or even harmonics from electrodes over occipital cortex (Supplementary Figure 3.4), the data was substantially less consistent with the subgroup relationships (yellow and green lines, Figure 5).

The current study uses 16 distinct wallpaper groups, while previous neuroimaging studies focused on a subset of 4 (Kohler et al., 2016, 2018). This represents a significant conceptual advance, because it makes it possible to investigate the complete subgroup hierarchy among the 17 groups and ask to what extent the hierarchy is reflected in brain activity. Our data provide a description of the visual system's response to the complete set of symmetries in the two-dimensional plane. We do not independently measure the response to  $P_1$ , but because each of the 16 other groups produce non-zero odd harmonic amplitudes (see Figure 2), we can conclude that the relationships between  $P_1$  and all other groups, where  $P_1$  is the subgroup, are also preserved by the visual system. The subgroup relationships are in many cases not obvious perceptually, and most participants had no knowledge of group theory. Thus, the visual system's ability to preserve the subgroup hierarchy does not depend on explicit knowledge of the relationships. Previous brain-imaging studies have found evidence of parametric responses with the number of reflection symmetry folds

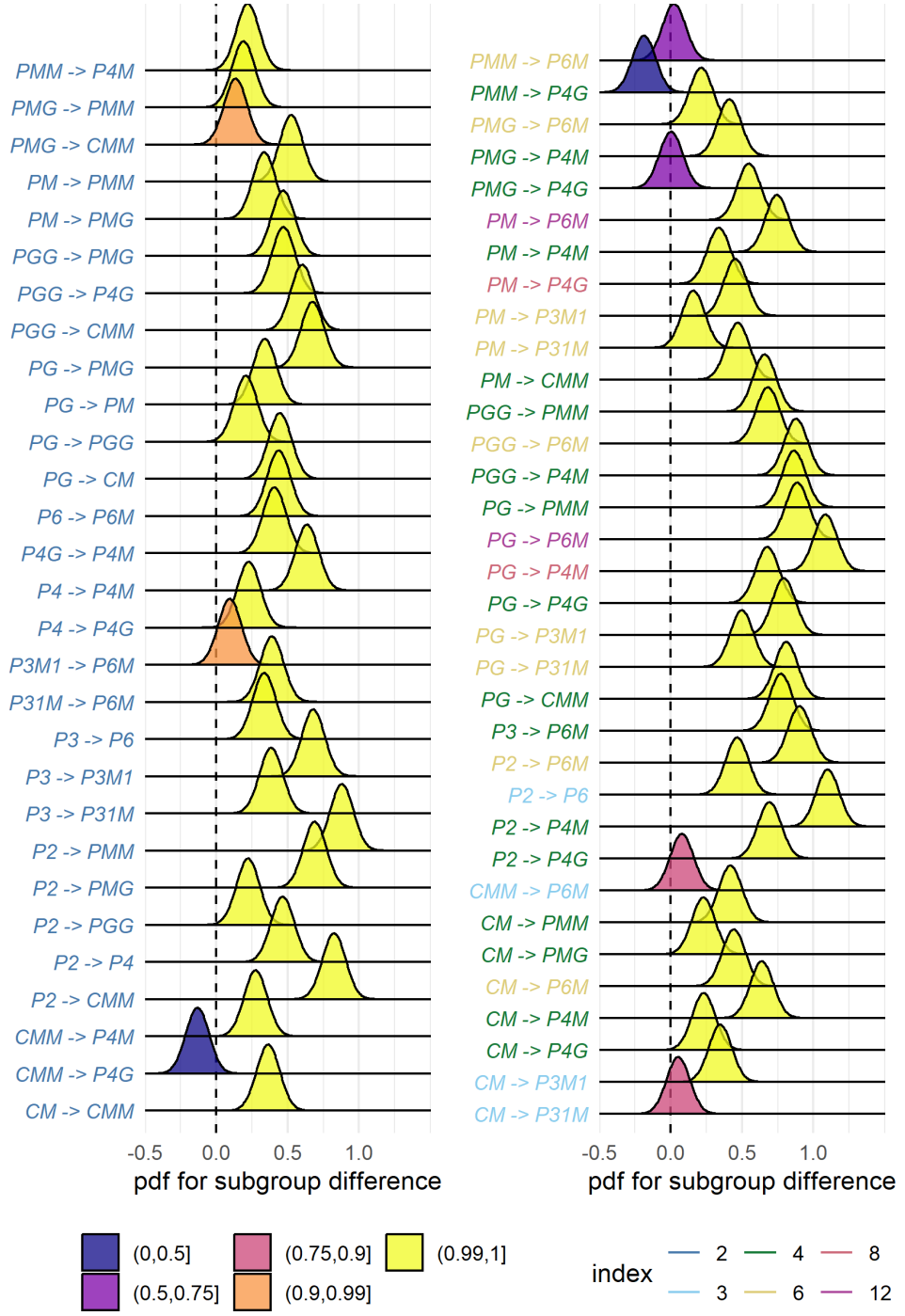


Figure 3: Posterior distributions for the difference in mean SSVEP RMS amplitude. Colour coding of the text indicates the index of the subgroup, while the colour of the filled distribution relates to the conditional probability that the difference in means is greater than zero. We can see that 55/63 subgroup relationships have  $p(\Delta|data) > 0.99$ .

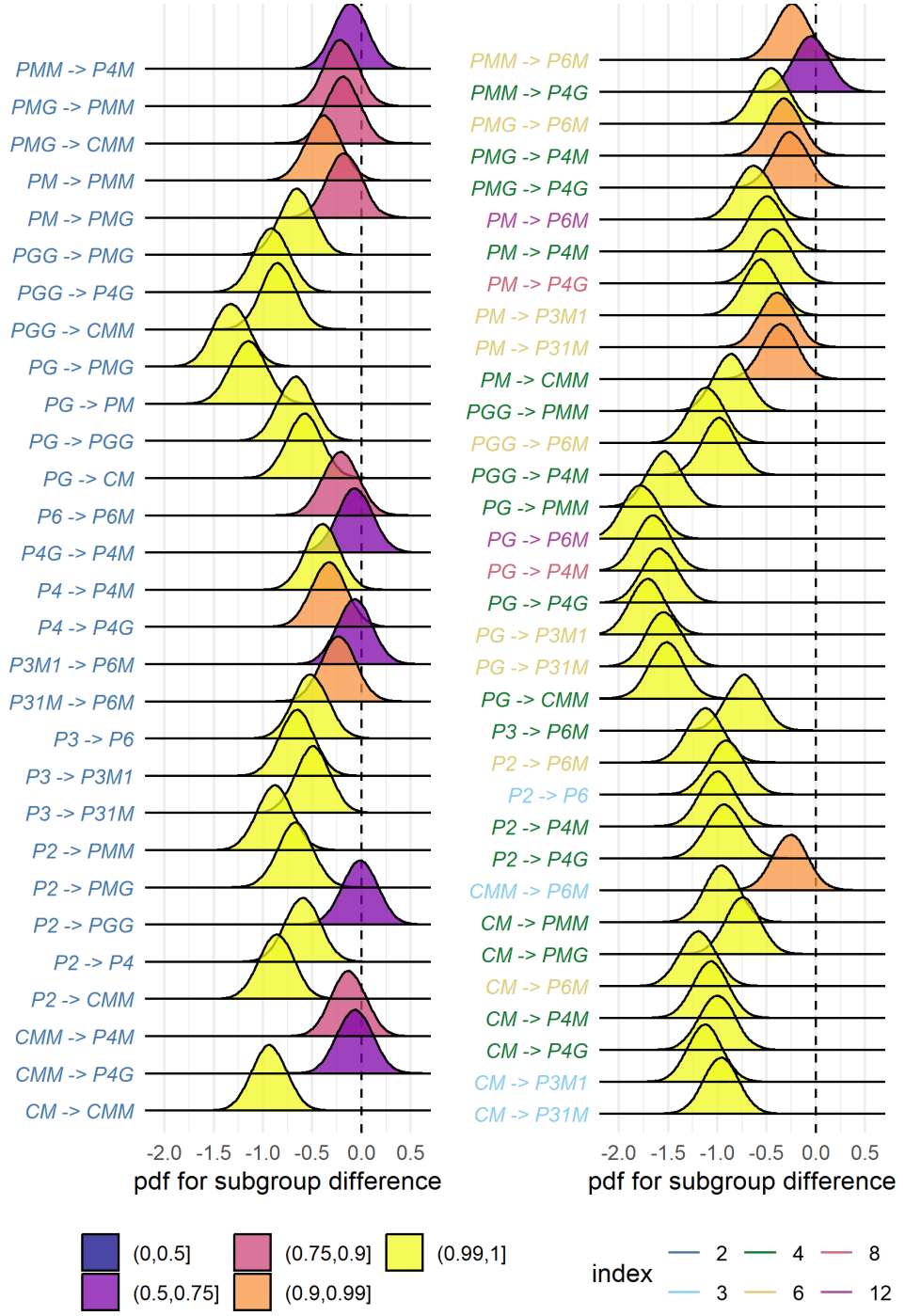


Figure 4: Posterior distributions for the difference in mean symmetry detection threshold durations. Colour coding of the text indicates the index of the subgroup, while the colour of the filled distribution relates to the conditional probability that the difference in means is greater than zero. We can see that 43/63 subgroup relationships have  $p(\Delta|data) > 0.99$ .

Keefe et al. (2018); Sasaki et al. (2005); Makin et al. (2016) and with the order of rotation symmetry Kohler et al. (2016). Our study is the first demonstration that the brain encodes symmetry in this parametric fashion across every possible combination of different *symmetry types*, and that this parametric encoding is also reflected in behavior. Previous behavioral experiments have shown that although naïve observers can distinguish many of the wallpaper groups (Landwehr, 2009), they tend to sort exemplars into fewer (4-12) sets than the number of wallpaper groups, often placing exemplars from different wallpaper groups in the same set (Clarke et al., 2011). The two-interval forced choice approach we use in the current psychophysical experiment makes it possible to directly compare symmetry detection thresholds to the subgroup hierarchy, and reveals that not only can the 17 wallpaper groups be distinguished based on behavioral data, behavior largely follows the subgroup hierarchy.

A large literature exists on the *Sustained Posterior Negativity* (SPN), a characteristic negative-going waveform that is known to reflect responses to symmetry and other forms of regularity and structure (Makin et al., 2016). The SPN scales with the proportion of reflection symmetry in displays that contain a mixture of symmetry and noise Makin et al. (2020); Palumbo et al. (2015), and both reflection, rotation and translation can produce a measurable SPN Makin et al. (2013). It has recently been demonstrated that a holographic model of regularity (van der Helm and Leeuwenberg, 1996), can predict both SPN amplitude (Makin et al., 2016) and perceptual discrimination performance (Nucci and Wagemans, 2007) for dot patterns that contain symmetry and other types of regularity. The available evidence suggests that the SPN and our SSVEP measurements are two distinct methods of isolating the same symmetry-related brain response: When observed in the time-domain, the symmetry-selective odd-harmonic responses produce similarly sustained waveforms (see Figure 2), odd-harmonic SSVEP responses can be measured for dot patterns similar to those used to measure the SPN (Norcia et al., 2002), and the one event-related study that has been published on the wallpaper groups produced SPN-like waveforms (Kohler et al., 2018). Future work should more firmly establish the connection and determine if the SPN can capture similarly precise symmetry responses as the SSVEPs presented here. It would also be worthwhile to ask if and how  $W$  can be computed for our random-noise based wallpaper textures where combinations of symmetries tile the plane.

We observe a reliable correlation between our brain imaging and psychophysical data. This suggests that the two measurements reflect the same underlying symmetry representations in visual cortex. It should be noted that the correlation is relatively modest ( $R^2 = 0.44$ ). This may be partly due to the fact that different individuals participated in the two experiments. It may also be related to the fact that participants were not doing a symmetry-related task during the SSVEP experiment, but instead monitored the stimuli for brief changes in contrast that occurred twice per trial (see Methods). Previous brain imaging studies have found enhanced reflection symmetry responses when participants performed a symmetry-related task (Makin et al., 2020; Sasaki et al., 2005; Keefe et al., 2018). It is possible that adding a symmetry-related task to our SSVEP experiment would have produced measurements that reflected subgroup relationships to an even higher extent than what we observed. On the other hand, our results are already close to ceiling (see Figure 5) and adding a symmetry-related task may simply enhance SSVEP ampli-

tudes overall without improving the discriminability of individual groups, as has been observed for reflection by Keefe et al. (2018). Task-driven processing may be important for detecting symmetries that have been subject to perspective distortion, as suggested by SPN measurements (Makin et al., 2015) and somewhat less clearly in a subsequent functional MRI study (Keefe et al., 2018). Future work in which behavioral and brain imaging data are collected from the same participants, and task is manipulated in the SSVEP experiment, will help further establish the connection between the two measurements, and elucidate the potential contribution of task-related top-down processing to the current results.

We also find an effect of index for both our brain imaging measurements and our symmetry detection thresholds. This means that the visual system not only represents the hierarchical relationship captured by individual subgroups, but also distinguishes between subgroups depending on how many times the subgroup is repeated in the supergroup, with more repetitions leading to larger pairwise differences. Our measured effect of index is relatively weak. This is perhaps because the index analysis does not take into account the *type* of isometries that differentiate the subgroup and supergroup. The effect of symmetry type can be observed by contrasting the measured SSVEP amplitudes and detection thresholds for groups *PM* and *PG* in Figure 2. The two groups are comparable except *PM* contains reflection and *PG* contains glide reflection, and the former clearly elicits higher amplitudes and lower thresholds. An important goal for future work will be to map out how different symmetry types contribute to the representational hierarchy.

The correspondence between responses in the visual system and group theory that we demonstrate here, may reflect a form of implicit learning that depends on the structure of the natural world. The environment is itself constrained by physical forces underlying pattern formation and these forces are subject to multiple symmetry constraints (Hoyle, 2006). The ordered structure of responses to wallpaper groups could be driven by a central tenet of neural coding, that of efficiency. If coding is to be efficient, neural resources should be distributed to capture the structure of the environment with minimum redundancy considering the visual geometric optics, the capabilities of the subsequent neural coding stages and the behavioral goals of the organism (Attneave, 1954; Barlow, 1961; Laughlin, 1981; Geisler et al., 2009). Early work within the efficient coding framework suggested that natural images had a  $1/f$  spectrum and that the corresponding redundancy between pixels in natural images could be coded efficiently with a sparse set of oriented filter responses, such as those present in the early visual pathway (Field, 1987; Olshausen and Field, 1997). Our results suggest that the principle of efficient coding extends to a much higher level of structural redundancy – that of symmetries in visual images.

The 17 wallpaper groups are completely regular, and relatively rare in the visual environment, especially when considering distortions due to perspective (see above) and occlusion. Near-regular textures, however, abound in the visual world, and can be modeled as deformed versions of the wallpaper groups (Liu et al., 2004). The correspondence between visual cortex responses and group theory demonstrated here may indicate that the visual system represents visual textures using a similar scheme, with the wallpaper groups serving as anchor points in representational space. This framework resembles norm-based encoding strategies that have been proposed for other stimulus classes, most notably faces (Leopold et al., 2006), and leads to the prediction that

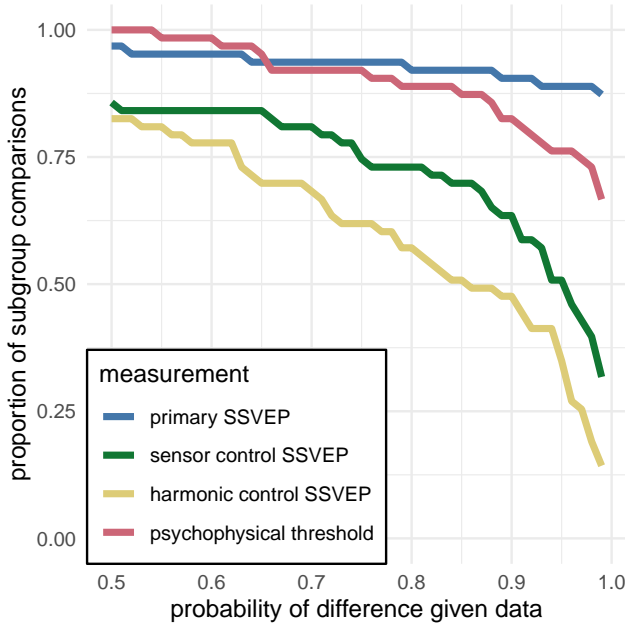


Figure 5: This plot shows the proportion of subgroup relationships that satisfy  $p(\Delta > 0 | data) > x$ . We can see that if we take  $x = 0.95$  as our threshold, the subgroup relationships are preserved in  $56/63 = 89\%$  and  $48/63 = 76\%$  of the comparisons for the primary SSVEP and threshold duration datasets, respectively. This compares to the  $32/63 = 51\%$  and  $22/63 = 35\%$  for the SSVEP control datasets.

adaptation to wallpaper patterns should distort perception of near-regular textures, similar to the aftereffects found for faces (Webster and MacLin, 1999). Field biologists have demonstrated that animals respond more strongly to exaggerated versions of a learned stimulus, referred to as “supernormal” stimuli (Tinbergen, 1953). In the norm-based encoding framework, wallpaper groups can be considered *supertextures*, exaggerated examples of the near-regular textures common in the natural world. If non-human animals employ a similar encoding strategy, they would be expected to be sensitive to symmetries in wallpaper groups. Recent functional MRI work in macaque monkeys offer some support for that: Macaque visual cortex responds parametrically to reflection and rotation symmetries in wallpaper groups, and the set of brain areas involved largely overlap those observed to be sensitive to symmetry in humans (Audurier et al., 2021). In human societies, visual artists may consciously or unconsciously create supernormal stimuli, to capture the essence of the subject and evoke strong responses in the audience (Ramachandran and Hirstein, 1999). Wallpaper groups are visually compelling, and symmetries have been widely used in human artistic expression going back to the Neolithic age (Jablan, 2014). If wallpapers are in fact supertextures, this prevalence may be a direct result of the strategy the human visual system has adopted for texture encoding.

## Participants

Twenty-five participants (11 females, mean age  $28.7 \pm 3.3$ ) took part in the EEG experiment. Their informed consent was obtained before the experiment under a protocol that was approved by the Institutional Review Board of Stanford University. 11 participants (8 females, mean age

316  $20.73 \pm 1.21$ ) took part in the psychophysics experiment. All participants had normal or corrected-  
317 to-normal vision. Their informed consent was obtained before the experiment under a protocol  
318 that was approved by the University of Essex's Ethics Committee. There was no overlap in  
319 participants between the EEG and psychophysics experiments.

## 320 Stimulus Generation

321 Exemplars from the different wallpaper groups were generated using a modified version of the  
322 methodology developed by Clarke and colleagues (Clarke et al., 2011) that we have described in de-  
323 tail elsewhere (Kohler et al., 2016). Briefly, exemplar patterns for each group were generated from  
324 random-noise textures, which were then repeated and transformed to cover the plane, according  
325 to the symmetry axes and geometric lattice specific to each group. The use of noise textures as  
326 the starting point for stimulus generation allowed the creation of an almost infinite number of  
327 distinct exemplars of each wallpaper group. To make individual exemplars as similar as possible  
328 we replaced the power spectrum of each exemplar with the median across exemplars within a  
329 group. We then generated control exemplars that had the same power spectrum as the exemplar  
330 images by randomizing the phase of each exemplar image. The phase scrambling eliminates ro-  
331 tation, reflection and glide-reflection symmetries within each exemplar, but the phase-scrambled  
332 images inherit the spectral periodicity arising from the periodic tiling. This means that all  
333 control exemplars, regardless of which wallpaper group they are derived from, are transformed  
334 into another symmetry group, namely  $P_1$ .  $P_1$  is the simplest of the wallpaper groups and contains  
335 only translations of a region whose shape derives from the lattice. Because the different wallpaper  
336 groups have different lattices,  $P_1$  controls matched to different groups have different power spectra.  
337 Our experimental design takes these differences into account by comparing the neural responses  
338 evoked by each wallpaper group to responses evoked by the matched control exemplars.

## 339 Stimulus Presentation

340 Stimulus Presentation. For the EEG experiment, the stimuli were shown on a 24.5" Sony Trimas-  
341 ter EL PVM-2541 organic light emitting diode (OLED) display at a screen resolution of  $1920 \times 1080$   
342 pixels, 8-bit color depth and a refresh rate of 60 Hz, viewed at a distance of 70 cm. The mean  
343 luminance was  $69.93 \text{ cd/m}^2$  and contrast was 95%. The diameter of the circular aperture in  
344 which the wallpaper pattern appeared was  $13.8^\circ$  of visual angle presented against a mean lumi-  
345 nance gray background. Stimulus presentation was controlled using in-house software. For the  
346 psychophysics experiment, the stimuli were shown on a  $48 \times 27 \text{ cm}$  VIEWPixx/3D LCD Display  
347 monitor, model VPX-VPX-2005C, resolution  $1920 \times 1080$  pixels, with a viewing distance of ap-  
348 proximately 40cm and linear gamma. Stimulus presentation was controlled using MatLab and  
349 Psychtoolbox-3 (Kleiner et al., 2007; Brainard, 1997). The diameter of the circular aperture for  
350 the stimuli was  $21.5^\circ$ .

351 EEG Procedure

352 Visual Evoked Potentials were measured using a steady-state design, in which  $P_1$  control images  
353 alternated with exemplar images from each of the 16 other wallpaper groups. Exemplar images  
354 were always preceded by their matched  $P_1$  control image. A single 0.83 Hz stimulus cycle consisted  
355 of a control  $P_1$  image followed by an exemplar image, each shown for 600 ms. A trial consisted of 10  
356 such cycles (12 sec) over which 10 different exemplar images and matched controls from the same  
357 rotation group were presented. For each group type, the individual exemplar images were always  
358 shown in the same order within the trials. Participants initiated each trial with a button-press,  
359 which allowed them to take breaks between trials. Trials from a single wallpaper group were  
360 presented in blocks of four repetitions, which were themselves repeated twice per session, and  
361 shown in random order within each session. To control fixation, the participants were instructed  
362 to fixate a small white cross in the center of display. To control vigilance, a contrast dimming  
363 task was employed. Two times per trial, an image pair (control  $P_1$  plus exemplar) was shown  
364 at reduced contrast. Participants were instructed to press a button on a response pad whenever  
365 they noticed a contrast change. Reaction times were not taken into account and participants were  
366 told to respond at their own pace while being as accurate as possible. We adjusted the reduction  
367 in contrast such that average accuracy for each participant was kept at 85% correct, in order to  
368 keep the difficulty of the vigilance task at a constant level.

369 Psychophysics Procedure

370 The experiment consisted of 16 blocks, one for each of the wallpaper groups (excluding  $P_1$ ). We  
371 used a two-interval forced choice approach. In each trial, participants were presented with two  
372 stimuli (one of which was the wallpaper group for the current block of trials, the other being  $P_1$ ),  
373 one after the other (inter-stimulus interval of 700ms). After each stimulus had been presented, it  
374 was masked with white noise for 300ms. After both stimuli had been presented, participants made  
375 a response on the keyboard to indicate whether they thought the first or second image contained  
376 more symmetry. Each block started with 10 practice trials, (stimulus display duration of 500ms)  
377 to allow participants to familiarise themselves with the current block's wallpaper pattern. If they  
378 achieved an accuracy of 9/10 in these trials they progressed to the rest of the block, otherwise  
379 they carried out another set of 10 practise trials. This process was repeated until the required  
380 accuracy of 9/10 was obtained. The rest of the block consisted of four interleaved staircases (using  
381 the QUEST algorithm (Watson and Pelli, 1983), full details given in the SI) of 30 trials each. On  
382 average, a block of trials took around 10 minutes to complete.

383 EEG Acquisition and Preprocessing

384 Steady-State Visual Evoked Potentials (SSVEPs) were collected with 128-sensor HydroCell Sensor  
385 Nets (Electrical Geodesics, Eugene, OR) and were band-pass filtered from 0.3 to 50 Hz. Raw data  
386 were evaluated off line according to a sample-by-sample thresholding procedure to remove noisy  
387 sensors that were replaced by the average of the six nearest spatial neighbors. On average, less  
388 than 5% of the electrodes were substituted; these electrodes were mainly located near the forehead

389 or the ears. The substitutions can be expected to have a negligible impact on our results, as the  
390 majority of our signal can be expected to come from electrodes over occipital, temporal and parietal  
391 cortices. After this operation, the waveforms were re-referenced to the common average of all  
392 the sensors. The data from each 12s trial were segmented into five 2.4 s long epochs (i.e., each of  
393 these epochs was exactly 2 cycles of image modulation). Epochs for which a large percentage of  
394 data samples exceeding a noise threshold (depending on the participant and ranging between 25  
395 and 50  $\mu$ V) were excluded from the analysis on a sensor-by-sensor basis. This was typically the  
396 case for epochs containing artifacts, such as blinks or eye movements. Steady-state stimulation  
397 will drive cortical responses at specific frequencies directly tied to the stimulus frequency. It is  
398 thus appropriate to quantify these responses in terms of both phase and amplitude. Therefore, a  
399 Fourier analysis was applied on every remaining epoch using a discrete Fourier transform with a  
400 rectangular window. The use of two-cycle long epochs (i.e., 2.4 s) was motivated by the need to  
401 have a relatively high resolution in the frequency domain,  $\delta f = 0.42$  Hz. For each frequency bin,  
402 the complex-valued Fourier coefficients were then averaged across all epochs within each trial.  
403 Each participant did two sessions of 8 trials per condition, which resulted in a total of 16 trials  
404 per condition.

#### 405 SSVEP Analysis

406 Response waveforms were generated for each group by selective filtering in the frequency do-  
407 main. For each participant, the average Fourier coefficients from the two sessions were averaged  
408 over trials and sessions. The SSVEP paradigm we used allowed us to separate symmetry-related  
409 responses from non-specific contrast transient responses. Previous work has demonstrated that  
410 symmetry-related responses are predominantly found in the odd harmonics of the stimulus fre-  
411 quency, whereas the even harmonics consist mainly of responses unrelated to symmetry, that  
412 arise from the contrast change associated with the appearance of the second image (Norcia et al.,  
413 2002; Kohler et al., 2016). This functional distinction of the harmonics allowed us to generate  
414 a single-cycle waveform containing the response specific to symmetry, by filtering out the even  
415 harmonics in the spectral domain, and then back-transforming the remaining signal, consisting  
416 only of odd harmonics, into the time-domain. For our main analysis, we averaged the odd har-  
417 monic single-cycle waveforms within a six-electrode region of interest (ROI) over occipital cortex  
418 (electrodes 70, 74, 75, 81, 82, 83). These waveforms, averaged over participants, are shown in  
419 Figure 2. The same analysis was done for the even harmonics and for the odd harmonics within a  
420 six electrode ROI over parietal cortex (electrodes 53, 54, 61, 78, 79, 86; see Supplementary Figure  
421 1.1). The root-mean square values of these waveforms, for each individual participant, were used  
422 to determine whether each of the wallpaper subgroup relationships were preserved in the brain  
423 data.

#### 424 Defining the list of subgroup relationships

425 In order to get the complete list of subgroup relationships, we digitized Table 4 from Coxeter  
426 (Coxeter and Moser, 1972) (shown in Supplementary Table 1.2). After removing identity rela-  
427 tionships (i.e. each group is a subgroup of itself) and the three pairs of wallpaper groups that are

428 subgroups of each other (e.g. *PM* is a subgroup of *CM*, and *CM* is a subgroup of *PM*) we were left  
429 with a total of 63 unambiguous subgroups that were included in our analysis.

## 430 Bayesian Analysis of SSVEP and Psychophysical data

431 Bayesian analysis was carried out using R (v3.6.1) (R Core Team, 2019) with the `brms` package  
432 (v2.9.0) (Bürkner, 2017) and rStan (v2.19.2 (Stan Development Team, 2019)). The data from each  
433 experiment were modelled using a Bayesian generalised mixed effect model with wallpaper group  
434 being treated as a 16-level factor, and random effects for participant. The SSVEP data and sym-  
435 metry detection threshold durations were modelled using log-normal distributions with weakly  
436 informative,  $\mathcal{N}(0, 2)$ , priors. After fitting the model to the data, samples were drawn from the  
437 posterior distribution of the two datasets, for each wallpaper group. These samples were then  
438 recombined to calculate the distribution of differences for each of the 63 pairs of subgroup and  
439 supergroup. These distributions were then summarised by computing the conditional probabil-  
440 ity of obtaining a positive (negative) difference,  $p(\Delta|\text{data})$ . For further technical details, please  
441 see the Supplementary Materials where the full R code, model specification, prior and posterior  
442 predictive checks, and model diagnostics, can be found.

## 443 References

- 444 Apthorp, D. and Bell, J. (2015). Symmetry is less than  
445 meets the eye. *Current Biology*, 25(7):R267–R268.
- 446 Attneave, F. (1954). Some informational aspects of  
447 visual perception. *Psychol Rev*, 61(3):183–93.
- 448 Audurier, P., Héjja-Brichard, Y., Castro, V. D.,  
449 Kohler, P. J., Norcia, A. M., Durand, J.-B., and  
450 Cottreau, B. R. (2021). Symmetry processing  
451 in the macaque visual cortex. *bioRxiv*, page  
452 2021.03.13.435181. Publisher: Cold Spring Harbor  
453 Laboratory Section: New Results.
- 454 Barlow, H. B. (1961). Possible principles underlying the  
455 transformations of sensory messages, pages 217–234.  
456 MIT Press.
- 457 Brainard, D. H. (1997). Spatial vision. *The psychophysics toolbox*, 10:433–436.
- 458 Bürkner, P.-C. (2017). Advanced bayesian multilevel  
459 modeling with the r package brms. *arXiv preprint arXiv:1705.11123*.
- 460 Clarke, A. D. F., Green, P. R., Halley, F., and  
461 Chantler, M. J. (2011). Similar symmetries: The  
462 role of wallpaper groups in perceptual texture sim-  
463 ilarity. *Symmetry*, 3(4):246–264.
- 464 Cohen, E. H. and Zaidi, Q. (2013). Symmetry in con-  
465 text: Salience of mirror symmetry in natural pat-  
466 terns. *Journal of vision*, 13(6).
- 467 Coxeter, H. S. M. and Moser, W. O. J. (1972). *Gen-  
468 erators and relations for discrete groups*. Ergebnisse  
469 der Mathematik und ihrer Grenzgebiete ; Bd. 14.  
470 Springer-Verlag, Berlin, New York.
- 471 Fedorov, E. (1891). Symmetry in the plane. In *Za-  
472 piski Imperatorskogo S. Peterburgskogo Mineralogichesko-  
473 go Obshchestva [Proc. S. Peterb. Mineral. Soc.]*, volume 2,  
474 pages 345–390.
- 475 Field, D. J. (1987). Relations between the statistics  
476 of natural images and the response properties of  
477 cortical cells. *J Opt Soc Am A*, 4(12):2379–94.
- 478 Geisler, W. S., Najemnik, J., and Ing, A. D. (2009). Opt-  
479 imal stimulus encoders for natural tasks. *Journal  
480 of Vision*, 9(13):17–17.
- 481 Giurfa, M., Eichmann, B., and Menzel, R. (1996).  
482 Symmetry perception in an insect. *Nature*,  
483 382(6590):458–461. Number: 6590 Publisher: Na-  
484 ture Publishing Group.
- 485 Hamada, J. and Ishihara, T. (1988). Complexity and  
486 goodness of dot patterns varying in symmetry. *Psy-  
487 chological Research*, 50(3):155–161.

- 490 Hoyle, R. B. (2006). *Pattern formation: an introduction to methods*. Cambridge University Press.
- 491 532
- 492 Jablan, S. V. (2014). *Symmetry, Ornament and Modularity*. World Scientific Publishing Co Pte Ltd, Singapore, SINGAPORE.
- 493 533 534 535 536
- 495 Keefe, B. D., Gouws, A. D., Sheldon, A. A., Vernon, R. J. W., Lawrence, S. J. D., McKeefry, D. J., Wade, A. R., and Morland, A. B. (2018). Emergence of symmetry selectivity in the visual areas of the human brain: fMRI responses to symmetry presented in both frontoparallel and slanted planes. *Human Brain Mapping*, 39(10):3813–3826.
- 496 500 501 502 503 504 505 506 507 508 509 510 511 512 513 514 515 516 517 518 519 520 521 522 523 524 525 526 527 528 529 530 531 532 533 534 535 536 537 538 539 540 541 542 543 544 545 546 547 548 549 550 551 552 553 554 555 556 557 558 559 560 561 562 563 564 565 566 567 568 569 570 571
- 490 Hoyle, R. B. (2006). *Pattern formation: an introduction to methods*. Cambridge University Press.
- 491 532
- 492 Jablan, S. V. (2014). *Symmetry, Ornament and Modularity*. World Scientific Publishing Co Pte Ltd, Singapore, SINGAPORE.
- 493 533 534 535 536
- 495 Keefe, B. D., Gouws, A. D., Sheldon, A. A., Vernon, R. J. W., Lawrence, S. J. D., McKeefry, D. J., Wade, A. R., and Morland, A. B. (2018). Emergence of symmetry selectivity in the visual areas of the human brain: fMRI responses to symmetry presented in both frontoparallel and slanted planes. *Human Brain Mapping*, 39(10):3813–3826.
- 496 500 501 502 503 504 505 506 507 508 509 510 511 512 513 514 515 516 517 518 519 520 521 522 523 524 525 526 527 528 529 529 530 531 532 533 534 535 536 537 538 539 539 540 541 542 543 544 545 546 547 548 549 549 550 551 552 553 554 555 556 557 558 559 559 560 561 562 563 564 565 566 567 568 569 569 570 571
- Liu, Y., Lin, W.-C., and Hays, J. (2004). Near-regular texture analysis and manipulation. In *ACM Transactions on Graphics (TOG)*, volume 23, pages 368–376. ACM.
- Mach, E. (1959). *The Analysis of Sensations (1897). English transl.*, Dover, New York.
- Makin, A. D. J., Rampone, G., and Bertamini, M. (2015). Conditions for view invariance in the neural response to visual symmetry. *Psychophysiology*, 52(4):532–543. eprint: <https://onlinelibrary.wiley.com/doi/pdf/10.1111/psyp.12365>.
- Makin, A. D. J., Rampone, G., Morris, A., and Bertamini, M. (2020). The Formation of Symmetrical Gestalts Is Task-Independent, but Can Be Enhanced by Active Regularity Discrimination. *Journal of Cognitive Neuroscience*, 32(2):353–366.
- Makin, A. D. J., Rampone, G., Pecchinenda, A., and Bertamini, M. (2013). Electrophysiological responses to visuospatial regularity. *Psychophysiology*, 50(10):1045–1055. eprint: <https://onlinelibrary.wiley.com/doi/pdf/10.1111/psyp.12082>.
- Makin, A. D. J., Rampone, G., Wright, A., Martinovic, J., and Bertamini, M. (2014). Visual symmetry in objects and gaps. *Journal of Vision*, 14(3):12–12. Publisher: The Association for Research in Vision and Ophthalmology.
- Makin, A. D. J., Wilton, M. M., Pecchinenda, A., and Bertamini, M. (2012). Symmetry perception and affective responses: A combined EEG/EMG study. *Neuropsychologia*, 50(14):3250–3261.
- Makin, A. D. J., Wright, D., Rampone, G., Palumbo, L., Guest, M., Sheehan, R., Cleaver, H., and Bertamini, M. (2016). An Electrophysiological Index of Perceptual Goodness. *Cerebral Cortex*, 26(12):4416–4434.
- Morris, M. R. and Casey, K. (1998). Female swordtail fish prefer symmetrical sexual signal. *Animal Behaviour*, 55(1):33–39.
- Møller, A. P. (1992). Female swallow preference for symmetrical male sexual ornaments. *Nature*, 357(6375):238–240.

- 572 Norcia, A. M., Appelbaum, L. G., Ales, J. M., Cottereau, B. R., and Rossion, B. (2015). The steady-state visual evoked potential in vision research: A review. *Journal of Vision*, 15(6):4–4. 617
- 576 Norcia, A. M., Candy, T. R., Pettet, M. W., Vildavski, V. Y., and Tyler, C. W. (2002). Temporal dynamics of the human response to symmetry. *Journal of Vision*, 2(2):132–139. 618  
619  
620
- 580 Nucci, M. and Wagemans, J. (2007). Goodness of Regularity in Dot Patterns: Global Symmetry, Local Symmetry, and Their Interactions. *Perception*, 36(9):1305–1319. Publisher: SAGE Publications Ltd STM. 621  
622  
623  
624  
625
- 585 Ogden, R., Makin, A. D. J., Palumbo, L., and Bertamini, M. (2016). Symmetry Lasts Longer Than Random, but Only for Brief Presentations. *i-Perception*, 7(6):2041669516676824. Publisher: SAGE Publications. 626  
627  
628  
629
- 590 Olshausen, B. A. and Field, D. J. (1997). Sparse coding with an overcomplete basis set: a strategy employed by v1? *Vision Res*, 37(23):3311–25. 630  
631  
632
- 593 Palmer, S. E. (1985). The role of symmetry in shape perception. *Acta Psychologica*, 59(1):67–90. 633  
634  
635
- 595 Palmer, S. E. (1991). Goodness, Gestalt, groups, and Garner: Local symmetry subgroups as a theory of figural goodness. In *The perception of structure: Essays in honor of Wendell R. Garner*, pages 23–39. American Psychological Association, Washington, DC, US. 636  
637  
638  
639
- 601 Palumbo, L., Bertamini, M., and Makin, A. (2015). Scaling of the extrastriate neural response to symmetry. *Vision Research*, 117:1–8. 640  
641  
642
- 604 Polya, G. (1924). Xii. Über die analogie der kristallsymmetrie in der ebene. *Zeitschrift für Kristallographie-Crystalline Materials*, 60(1):278–284. 643  
644  
645
- 607 R Core Team (2019). *R: A Language and Environment for Statistical Computing*. R Foundation for Statistical Computing, Vienna, Austria. 646  
647  
648
- 610 Ramachandran, V. S. and Hirstein, W. (1999). The science of art: A neurological theory of aesthetic experience. *Journal of Consciousness Studies*, 6(6–7):15–41. 649  
650  
651  
652
- 572 Rhodes, G., Proffitt, F., Grady, J. M., and Sumich, A. (1998). Facial symmetry and the perception of beauty. *Psychonomic Bulletin & Review*, 5(4):659–669.
- 576 Royer, F. L. (1981). Detection of symmetry. *Journal of Experimental Psychology: Human Perception and Performance*, 7(6):1186–1210.
- 580 Sasaki, Y., Vanduffel, W., Knutson, T., Tyler, C., and Tootell, R. (2005). Symmetry activates extrastriate visual cortex in human and nonhuman primates. *Proceedings of the National Academy of Sciences of the United States of America*, 102(8):3159–3163.
- 585 Schlüter, A., Parzefall, J., and Schlupp, I. (1998). Female preference for symmetrical vertical bars in male sailfin mollies. *Animal Behaviour*, 56(1):147–153.
- 590 Stan Development Team (2019). RStan: the R interface to Stan. R package version 2.19.2.
- 593 Swaddle, J. P. (1999). Visual signalling by asymmetry: a review of perceptual processes. *Philosophical Transactions of the Royal Society of London. Series B: Biological Sciences*. Publisher: The Royal Society.
- 595 Swaddle, J. P. and Cuthill, I. C. (1994). Preference for symmetric males by female zebra finches. *Nature*, 367(6459):165–166. Number: 6459 Publisher: Nature Publishing Group.
- 601 Tinbergen, N. (1953). *The herring gull's world: a study of the social behaviour of birds*. Frederick A. Praeger, Inc., Oxford, England.
- 607 Tyler, C. W., Baseler, H. A., Kontsevich, L. L., Likova, L. T., Wade, A. R., and Wandell, B. A. (2005). Predominantly extra-retinotopic cortical response to pattern symmetry. *Neuroimage*, 24(2):306–314.
- 610 van der Helm, P. A. and Leeuwenberg, E. L. J. (1996). Goodness of visual regularities: A nontransformational approach. *Psychological Review*, 103(3):429–456. Publisher: American Psychological Association.

- 653 von Fersen, L., Manos, C. S., Goldowsky, B., and Roitblat, H. (1992). Dolphin Detection and Conceptualization of Symmetry. In Thomas, J. A., Kastelein, R. A., and Supin, A. Y., editors, *Marine Mammal Sensory Systems*, pages 753–762. Springer US, Boston, MA.
- 659 Wagemans, J. (1998). Parallel visual processes in symmetry perception: Normality and pathology. *Documenta Ophthalmologica*, 95(3):359.
- 662 Wagemans, J., Van Gool, L., and d'Ydewalle, G. (1991). Detection of symmetry in tachistoscopically presented dot patterns: effects of multiple axes and skewing. *Perception & Psychophysics*, 50(5):413–27.
- 665 Watson, A. B. and Pelli, D. G. (1983). Quest: A bayesian adaptive psychometric method. *Perception & Psychophysics*, 33(2):113–120.
- 668 Webster, M. A. and MacLin, O. H. (1999). Figural aftereffects in the perception of faces. *Psychon Bull Rev*, 6(4):647–53.
- 671 Wright, D., Makin, A. D. J., and Bertamini, M. (2015). Right-lateralized alpha desynchronization during regularity discrimination: Hemispheric specialization or directed spatial attention? *Psychophysiology*, 52(5):638–647. eprint: <https://onlinelibrary.wiley.com/doi/pdf/10.1111/psyp.12399>.